Article

An Online Control Method of Reactive Power and Voltage Based on Mechanism–Data Hybrid Drive Model Considering Source–Load Uncertainty

Xu Huang [1], Guoqiang Zu [1], Qi Ding [1], Ran Wei [2], Yudong Wang [3,*] and Wei Wei [3,*]

[1] Chengdong Power Supply Branch, State Grid Tianjin Electric Power Company, Tianjin 300250, China
[2] State Grid Tianjin Electric Power Company, Tianjin 300010, China
[3] School of Electrical and Information Engineering, Tianjin University, Tianjin 300072, China
* Correspondence: wangyudong0727@tju.edu.cn (Y.W.); weiw@tju.edu.cn (W.W.)

Abstract: The uncertainty brought about by the high proportion of distributed generations poses great challenges to the operational safety of novel distribution systems. Therefore, this paper proposes an online reactive power and voltage control method that integrates source–load uncertainty and a mechanism–data hybrid drive (MDHD) model. Based on the concept of a mechanism and data hybrid drive, the mechanism-driven deterministic reactive power optimization strategy and the stochastic reactive power optimization strategy are used as training data. By training the data-driven CNN–GRU network model offline, the influence of source–load uncertainty on reactive power optimization can be effectively assessed. On this basis, according to the online source and load predicted data, the proposed hybrid-driven model can be applied to quickly obtain the reactive power optimization strategy to enable fast control of voltage. As observed in the case studies, compared with the traditional deterministic and stochastic reactive power optimization models, the hybrid-driven model not only satisfies the real-time requirement of online voltage control, but also has stronger adaptability to source–load uncertainty.

Keywords: source–load uncertainty; data-mechanical hybrid drive; reactive power optimization; CNN–GRU

1. Introduction

In recent years, with the concept of "carbon peak and carbon neutrality", the high proportion of renewable energy (e.g., solar and wind) access will become the fundamental feature and development trend of the novel power system [1]. However, the widespread connection of distributed generations and the increasing popularity of electric vehicles have made the source–load uncertainty of the power grid more and more obvious, which has aggravated the voltage violation risk caused by the randomness of power flow distribution and has posed a serious challenge to the reactive power and voltage control of the power system [2]. At the same time, with the improvement of digital informatization technology and the increase in the level of equipment automation, the novel distribution system also puts forward higher requirements for real-time control and adaptability to source–load uncertainty. The randomness of the source and load power makes it difficult to accurately predict, which also seriously reduces the reliability of power system control decisions. Current research usually adopts the Monte Carlo (MC) method to convert the deterministic power flow calculation in the traditional reactive power optimization model to probabilistic power flow in order to reasonably cope with the influence of source–load uncertainty on the reactive power optimization [3].

Ref. [4] proposed a linearization modeling method for on-load tap changers (OLTCs) and verified the effectiveness of the second-order cone programming (SOCP) model for solving reactive power optimization problems with OLTCs. Ref. [5] adopted a chance

constraint approach to convert the uncertainty problem into a deterministic problem, which effectively solved the problem of voltage control for the uncertainty of distributed energy resources (DERs). Ref. [6] adopted the MC method and scenario reduction technique to generate typical scenarios to deal with the stochastic optimal reactive power dispatch problem with uncertainties in load and DERs. Ref. [7] adopted a data-driven, distributionally robust optimization model to deal with the uncertainty of renewable generation, which, to a certain extent, effectively reduced the conservativeness of the results. Ref. [8] constructed a two-stage robust optimization model for the coordinated control of discrete and continuous reactive power compensation devices, in order to effectively address the influence of wind power uncertainty on a reactive power strategy; however, the model was complicated, and the computation time was long. The above reactive power and voltage control methods are mainly solved based on the mechanism-driven model of optimization theory, while in the novel distribution system, with a wide variety of devices, multi-source heterogeneous data and complex coupling relationships, the traditional solution driven by the mechanism model will lead to huge computational costs and even exceed the capability of the optimization solver. It is also difficult to meet the rapidity requirements for online reactive power and voltage control in distribution system.

In recent years, with the rapid development of artificial intelligence technology, data-driven methods have been widely used in the field of reactive power control. In Ref. [9], a distributed Q-learning algorithm was adopted to minimize active power loss while satisfying operational constraints, and it showed good adaptability and robustness under different operating conditions. Ref. [10] proposed a reactive power control method based on a deep deterministic policy gradient algorithm, in order to effectively solve the voltage violation problem in the active distribution network. Ref. [11] proposed a data-driven, two-stage, stochastic dynamic reactive power optimization model, which aimed to find the optimal solution under the worst-case probability distribution. In Ref. [12], a big data modeling method based on large-dimensional random matrix theory was proposed for reactive power optimization. Ref. [13] proposed a data-driven, multi-agent deep reinforcement learning (MADRL) model for voltage control. Since the data-driven reactive power optimization algorithm lacks prior knowledge as guidance, and the model itself has "black-box" characteristics, its performance largely depends on the quality of training data, and its reliability in practical applications cannot be effectively guaranteed. The model-data hybrid drive (MDHD) method combines the explicit principle of the mechanism model and the excellent fitting capability of the data model, which has become an important factor in refining of power system models [14]. Ref. [15] combined the linear power flow model based on physical equations and the data-driven error model to improve the accuracy of calculation results. Ref. [16] applied the model-data hybrid drive method to distribution line fault assessments. Ref. [17] used the frequency prediction results, which were calculated using the mechanism model, as the training input for the data model, in order to achieve the correction of the frequency prediction error. Ref. [18] proposed an MDHD modeling approach to generate accurate linear models for multiple energy flow (MEF) calculations. Considering the contradiction between model complexity and the computation speed of existing reactive power and voltage control methods, it is difficult to satisfy the real-time control requirements of novel distribution systems. Therefore, the application of an MDHD modeling method to the online control of the power grid is an effective solution. To summarize, in order to reasonably cope with the influence of source–load uncertainty on real-time voltage control, this paper proposes an MDHD model for online reactive power and voltage control. Mechanism-driven deterministic reactive power optimization results and stochastic reactive power optimization results are used as training data. The CNN–GRU network is trained offline and used for online control to achieve the fast correction of the deterministic reactive power optimization results, which takes into consideration the influence of source–load uncertainty on voltage control. Compared with the traditional deterministic and stochastic optimization models, the proposed MDHD model can better satisfy the real-time requirements, and shows a stronger adaptability to

source–load uncertainty, which has outstanding advantages in the online voltage control of novel distribution systems.

The remainder of this paper is organized as follows: Section 2 describes source–load uncertainty using the power prediction error, and constructs the source and load uncertainty model. Section 3 constructs the reactive power optimization model based on mixed integer SOCP. Section 4 proposes the online control method of reactive power and voltage based on MDHD, and specifies the implementation processes of the offline and online stages. Section 5 demonstrates the effectiveness and online application performance of the proposed method through simulation results. Section 6 concludes this paper.

2. Source–Load Uncertainty Model

2.1. Renewable Energy Uncertainty Model

Wind- and solar-based renewable energies have the characteristics of randomness and fluctuation, which has a significant influence on the decision making of power systems. Although the prediction technology for the output of wind turbine (WT) and photovoltaic (PV) systems has become increasingly sophisticated, the prediction results often cannot truly reflect the actual situation due to the influence of weather, geography and other factors [19]. Existing research results show that the output of WT and PV systems in a certain time period can be expressed as the sum of the predicted value and the prediction error [20,21]:

$$P_r(t) = P_r^{pre}(t) + \varepsilon_r(t) \tag{1}$$

where $P_r(t)$ and $P_r^{pre}(t)$ represent the actual and predicted values, respectively, of the WT or PV outputs in t time period; and $\varepsilon_t(t)$ represents the prediction error of the WT or PV outputs in that period. According to the central limit theorem, the prediction error obeys a normal distribution with mean 0 [22,23] (i.e., $\varepsilon_r \in N(0, \sigma_r^2)$). The standard deviation σ_r can be calculated by the following equation:

$$\sigma_r(t) = k_r P_r^{pre}(t) + \frac{1}{50}P_I \tag{2}$$

where P_I represents the installation capacity of WT or PV systems; and k_r is the WT or PV output prediction error coefficient. Considering the actual situation, the WT output prediction error coefficient is larger than that of the PV system.

2.2. Load Uncertainty Model

The load power is influenced by electricity behavior and has a certain randomness. Considering that the load prediction technology has developed significantly, but still cannot reflect the fluctuation of load power, in this paper, the actual load power P_{ld} is expressed as the sum of load power predicted value P_{ld}^{pre} and load power prediction error ΔP_{ld}. ΔP_{ld} is usually considered to follow a normal distribution with mean 0 (i.e., $\Delta P_{ld} \in N(0, \sigma_{ld}^2)$) [24]. The load uncertainty model can be expressed as follows:

$$P_{ld}(t) = P_{ld}^{pre}(t) + \Delta P_{ld}(t) \tag{3}$$

$$\sigma_{ld}(t) = \lambda P_{ld}^{pre}(t) \tag{4}$$

where $\sigma_{ld}(t)$ represents the standard deviation of the load power prediction error $\Delta P_{ld}(t)$ in t time period; $P_{ld}^{pre}(t)$ represents the load active power predicted value of that period; and λ is the proportional coefficient, which can be estimated using historical data.

Source–load uncertainty can be effectively calculated using the power prediction error model constructed above. This paper adopts the Latin Hypercube Sampling (LHS) method to generate simulation scenarios based on the probability distribution of the source–load prediction error for the subsequent stochastic reactive power optimization analysis. The LHS method can ensure that the samples cover the entire value space of the random

variables even when the number of samples is small. The specific steps are described in Ref. [25].

3. Reactive Power Optimization Model Based on Mixed Integer SOCP

3.1. The Objective Function

In this paper, discrete reactive power devices, such as *OLTCs*, capacitor banks and continuous devices, such as *SVCs*, were selected as a means of regulation to optimize system reactive power through collaborative scheduling. The reactive power optimization objective function was constructed with the goal of minimizing the system active power loss. Its form is shown in Equation (5):

$$\min \sum_{i,j \in \phi_{all}, i \neq j} \left(\frac{P_{ij}^2 + Q_{ij}^2}{U_i^2} \right) R_{ij} \tag{5}$$

where ϕ_{all} is the set of all nodes.

3.2. The Constraints

1. Distflow constraints [26]

$$\begin{cases} P_{ij} - R_{ij}I_{ij}^2 + P_j = P_{jk} \\ P_j = P_{j,DG} - P_{j,d} \end{cases} \tag{6}$$

$$\begin{cases} Q_{ij} - X_{ij}I_{ij}^2 + Q_j = Q_{jk} \\ Q_j = Q_{j,DG} + Q_{j,CB} + Q_{j,SVC} - Q_{j,d} \end{cases} \tag{7}$$

$$U_i^2 - U_j^2 = 2(R_{ij}P_{ij} + X_{ij}Q_{ij}) - (R_{ij}^2 + X_{ij}^2)I_{ij}^2 \tag{8}$$

$$I_{ij}^2 = (P_{ij}^2 + Q_{ij}^2)/U_i^2 \tag{9}$$

where P_{ij} and Q_{ij} represent the active and reactive power, respectively, of the sending end from bus i to j; P_j and Q_j represent the active and reactive power injection, respectively, at bus j; R_{ij} and X_{ij} represent the resistance and reactance, respectively, on branch ij; I_{ij} represents the current amplitude on branch ij; U_i represents the voltage amplitude of node i; $P_{j,DG}$ and $Q_{j,DG}$ represent the active and reactive power, respectively, of the distributed generations connected to node j; $Q_{j,CB}$ and $Q_{j,SVC}$ represent the compensating reactive power of the capacitor bank and *SVC*, respectively, connected to node j; and $P_{j,d}$ and $Q_{j,d}$ represent the active and reactive power, respectively, of the load connected to node j.

2. DG operation constraints:

$$0 \leq P_{j,DG} \leq P_{j,DG}^{\max} \tag{10}$$

$$-Q_{j,DG}^{\max} \leq Q_{j,DG} \leq Q_{j,DG}^{\max} \tag{11}$$

where $P_{j,DG}^{\max}$ and $Q_{j,DG}^{\max}$ represent the upper limits of the active and reactive power, respectively, of the distributed generations connected to node j.

3. Capacitor bank operation constraints:

$$Q_{j,CB} = d_j Q_{j,CB}^{step} \tag{12}$$

$$0 \leq d_j \leq n_{j,CB} \tag{13}$$

where $Q_{j,CB}^{step}$ represents the reactive power compensation of a set of capacitor bank; $n_{j,CB}$ represents the maximum switching sets of the capacitor bank; and d_j represents the actual switching sets of the capacitor bank, which is an integer variable.

4. *SVC* operation constraints:

$$Q_{j,SVC}^{\min} \le Q_{j,SVC} \le Q_{j,SVC}^{\max} \tag{14}$$

where $Q_{i,SVC}^{\min}$ and $Q_{i,SVC}^{\max}$ represent the lower and upper limits, respectively, of reactive power compensation of the *SVC* connected to the node j.

5.　　*OLTC* operation constrains:

$$U_i = k_{ij}U_j \tag{15}$$

$$k_{ij} = k_{ij}^{\min} + \Delta k_{ij} \sum_{n=0}^{N_{ij}} 2^n \lambda_{ij,n} \tag{16}$$

$$\sum_{n=0}^{N_{ij}} 2^n \lambda_{ij,n} - K_{ij}^{\max} \le 0 \tag{17}$$

The *OLTC* is represented in binary code. Where $\lambda_{ij,n}$ is 0–1 integer variable; N_{ij} is a constant, and its value represents the number of binary bits needed to express the maximum position of the *OLTC*; $K_{ij}^{\max}$ represents the maximum adjustable position of the *OLTC*; k_{ij} represents the *OLTC* adjustable ratio; and $k_{ij}^{\min}$ and Δk_{ij} represent the lower limit and the adjustment step of k_{ij}, respectively.

6.　　Security constraints:

$$U_{i,\min} \le U_i \le U_{i,\max} \tag{18}$$

$$I_{ij,\min} \le I_{ij} \le I_{ij,\max} \tag{19}$$

where $U_{i,\min}$ and $U_{i,\max}$ represent the lower and upper limits of the node voltage amplitude, respectively; and $l_{ij,\min}$ and $l_{ij,\max}$ represent the lower and upper limits of the branch circuit current amplitude, respectively.

3.3. Second-Order Cone Relaxation

According to the characteristics of *SOCP* [27], $u_i = U_i^2$, $l_{ij} = I_{ij}^2$, and then a second-order cone relaxation of the non-linear power flow constraints in Equations (6)–(9) can be calculated, which can be converted into the following constraints:

$$P_{ij} - R_{ij}l_{ij} + P_j = P_{jk} \tag{20}$$

$$Q_{ij} - X_{ij}l_{ij} + Q_j = Q_{jk} \tag{21}$$

$$u_i - u_j = 2(R_{ij}P_{ij} + X_{ij}Q_{ij}) - (R_{ij}^2 + X_{ij}^2)l_{ij} \tag{22}$$

$$l_{ij} = (P_{ij}^2 + Q_{ij}^2)/u_i \tag{23}$$

and then a further relaxation of Equation (23) is made, which can be represented as the standard form of *SOC* constraint:

$$\left\| \begin{matrix} 2P_{ij} \\ 2Q_{ij} \\ l_{ij} - u_i \end{matrix} \right\|_2 \le l_{ij} + u_i \tag{24}$$

After the above cone processing, the original non-convex constraints can be converted into linear constraints. In this paper, due to the inclusion of discrete variables, the reactive power optimization model becomes a mixed integer second-order cone programming model, which can be effectively solved by using commercial software, such as Cplex.

4. Online Control Model of Reactive Power and Voltage Based on MDHD

4.1. CNN–GRU Network

In this paper, a CNN–GRU network was constructed as the data-driven model. The network used CNN to extract data and input the results into GRU, which was used to construct complex mapping relationships. The CNN–GRU network not only enables the full utilization of historical data, but also effectively improves the output accuracy [28].

The main role of the CNN–GRU model constructed in this paper was to correct the reactive power optimization strategy solved by the deterministic mechanism model under source–load uncertainty conditions. Considering that the stochastic optimization model can effectively reflect the influence of source–load uncertainty on the calculated results, its results were more reasonable compared to the deterministic optimization model. Therefore, the reactive power strategies solved by the deterministic optimization model at each operating moment of the system were taken as the input features, and the reactive power strategies solved by the stochastic optimization model were taken as the output labels. Moreover, considering that the stochastic optimization results depend on the degree of source–load uncertainty at each moment, the source and load prediction error coefficients at the corresponding moment were also used as input features.

The network training effect depends largely on the quality and format of the sample data, and the discrete data included in the reactive strategy will cause the network training accuracy to decrease. Therefore, this paper used a binary-coded method to process the discrete variables in input features and output labels [29]. Specifically, the *OLTC* was represented in *m*-bit binary codes, and the switching sets of the capacitor bank were represented in *n*-bit binary codes.

As a result, the input data of the CNN–GRU model was a single-channel grayscale image with the dimensions $(N + 3) \times 1 \times 1$. In the first dimension, 3 represents the number of prediction error coefficients for PVs, WTs and load power; and N represents the number of all adjustable variables in reactive power strategy. The value of N is as follows:

$$N = N_{OLTC} \cdot m + N_{CB} \cdot n + N_{SVC} \cdot 1 \tag{25}$$

where N_{OLTC}, N_{CB} and N_{SVC} represent the number of *OLTCs*, capacitor banks and *SVCs*, respectively, involved in reactive power control. The output data was a sequence with the dimensions $N \times 1$, which represents the corrected reactive power strategy by considering the source–load uncertainty, where each discrete device is coded in the same order as the input data.

By processing the input and output data as described above, the CNN–GRU network can be trained to map from deterministic reactive power optimization results to stochastic reactive power optimization results, thus taking into account the influence of source–load randomness on the reactive power optimization strategy.

4.2. Online Reactive Power and Voltage Control Model Based on MDHD

The online control method of reactive power and voltage based on the MDHD model was divided into two stages: offline training and online application. The implementation processes are shown in Figure 1. The offline stage mapped the relationship between the deterministic reactive power optimization results and the stochastic reactive power optimization results by training the CNN–GRU model, and applied the trained model directly to the online stage. This method can make voltage control faster and more accurate, while effectively handling source–load uncertainty. Its specific implementation processes are as follows. The offline training stage included the following steps:

(1) Based on the historical data, the source and load prediction error coefficients at a certain time were determined, and then the source and load uncertainty models were constructed. On this basis, the LHS method was used to generate several groups of source and load scenarios.

(2) The deterministic reactive power optimization was carried out with each group of scenarios as boundary conditions in turn, and the results were statistically analyzed. The expected values of the positions of the *OLTC*, the switching sets of the capacitor bank, and the reactive power compensation of the *SVC* was taken as the reactive power control strategy obtained by stochastic optimization.

(3) Steps (1) and (2) were performed for the WT, PV and load historical power data, and the set of reactive power strategies were stored in the historical strategy library, denoted as $W = [W_1, W_2, \cdots, W_t, \cdots]$. W_t represents the reactive power control strategy obtained by the stochastic optimization model at time t.

(4) For the above WT, PV and load historical power data, the deterministic model based on mixed integer second-order cone programming was used for reactive power optimization. The set of reactive power control strategies obtained at each time was noted as $W' = [W'_1, W'_2, \cdots, W'_t, \cdots]$.

(5) The set of reactive power control strategies obtained from the deterministic optimization model and the set of source and load prediction error coefficients were spliced vertically as the input features, and the set of reactive power strategies obtained from the stochastic optimization model was used as output labels to construct the data sample set and train the CNN–GRU model. The discrete variables in W and W' were converted into a binary-coded form.

The online application stage was mainly conducted as follows:

(1) The WT, PV and load power for a future time was predicted and noted as $X^{pre} = [P^{pre}_{pv}, P^{pre}_{wt}, P^{pre}_{ld}]$. Where P^{pre}_{pv} was the predicted value of the PV output, P^{pre}_{wt} was the predicted value of the WT output and P^{pre}_{ld} was the predicted value of the load power.

(2) The predicted data X^{pre} was input into the deterministic reactive power optimization model to obtain the initial reactive power strategy W_{ini}.

(3) W_{ini} and the source and load prediction error coefficients at that time were input into the CNN–GRU model which had already been trained offline. The output W_{cor} was the corrected reactive power optimization strategy, considering the source–load uncertainty.

(4) The reactive power control strategy was decoded and sent into the grid to provide auxiliary decisions for the schedulers.
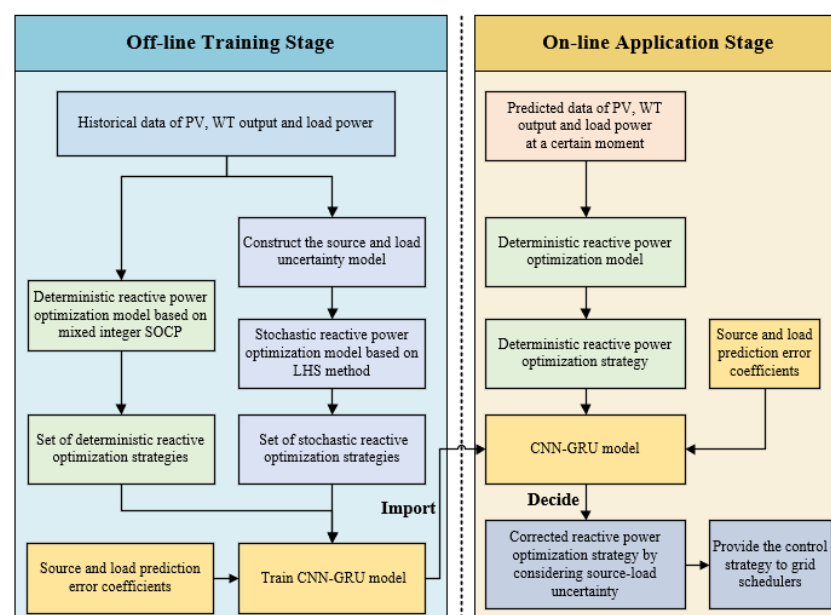
Figure 1. Implementation process of online reactive power and voltage control method based on MDHD model.

To verify the performance of the online reactive power and voltage control method based on the MDHD model proposed in this paper, MATLAB 2020a was used for simulation calculations, with an embedded deep learning toolbox and YALMIP optimization toolbox, and a Cplex 12.8 commercial solver was used for optimization solutions. The computer configuration was an Intel(R) Corei7-7700HQ with 2.8 GHz processor and 8 GB RAM.

5. Results and Discussion

In this section, a modified IEEE 33-node distribution system is taken as a case study to verify the feasibility and effectiveness of the voltage control method proposed above. The system structure is shown in Figure 2. Regulation equipment such as WTs, PV systems, *OLTCs*, *SVCs* and capacitor banks were added, and the specific parameter configurations are shown in Table 1. The system voltage reference was set to 12.66 KV and the power reference was set to 10 MVA. The parameters of the case system refer to Ref. [30], and the line parameters are shown in Appendix A. The upper and lower limits of the node voltage were set to 1.05 p.u. and 0.95 p.u, respectively. In addition, the WT and PV systems were operated in a constant power factor mode, and the relevant parameter configurations are shown in Table 2.
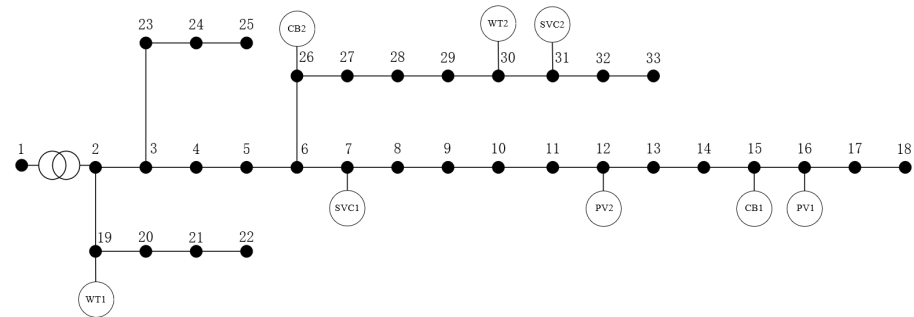
Figure 2. The structure of the case system.

Table 1. Regulation equipment parameters.

	Grid-Connected Position	**Range/kVar**	**Step/kVar**
CB1	15	[0, 800]	100
CB2	26	[0, 800]	
*SVC*1	7	[−100, 1200]	continuous
>*SVC*2	31	[−100, 1200]	
	Grid-connected Position	**Range**	**Step**
OLTC	1–2	[0.95, 1.05]	0.025

Table 2. PV and WT parameters.

	Grid-Connected Position	**Total Capacity/kW**	**Power Factor**
WT1	19	1000	
WT2	30	800	0.9
PV1	16	1000	
PV2	12	800	

5.1. Analysis of Offline Model Training

In this section, the predicted values of source and load from June to September in a certain place were selected as the input data of the WT and PV sources, and the load in the case, and the prediction interval was known to be 1 h, with a total of 2928 groups. Considering the strong randomness of actual wind speed, the WT output prediction error coefficient k_{wt} was taken as 15%, the PV output prediction error coefficient k_{pv} was taken as 10%, and the load power prediction error coefficient k_{ld} was taken as 5%. The sample

size of the LHS was set to 200. The reactive power strategies solved by the stochastic model at each time were used as output labels, and the reactive power strategies solved by the deterministic model were used as input features to train the CNN model, the GRU model and the CNN–GRU model. The specific training process is shown in Figure 3.
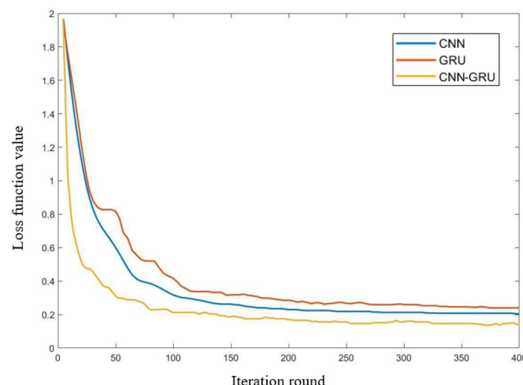
Figure 3. Training iteration process of different models.

The comparison of results in Table 3 shows that both the training performance and prediction accuracy of the CNN–GRU model were significantly superior to those of the CNN and GRU models. By the time the iteration reached 120 rounds, the loss function value of the CNN–GRU model was reduced to below 0.12. Additionally, the RMSE value of the CNN–GRU model on the test set was 0.4472. The above results fully demonstrate that the CNN–GRU model has better performance in processing multi-dimensional and time-series data, and can be selected as the data-driven model for the online control method of reactive power and voltage.

Table 3. Prediction effect of different models.

	RMSE
CNN	0.5164
GRU	0.5462
CNN–GRU	0.4472

5.2. Analysis of Online Application Performance

1. Analysis of Online Application Effective

To further illustrate the effectiveness of the proposed hybrid-driven model applied to the online reactive power and voltage control, for a group of source and load predicted values at a certain time, the deterministic model, the stochastic model and the hybrid-driven model were used for reactive power optimization. Table 4 shows the reactive power strategies and the computation time obtained by solving the three models.

Table 4. Comparison of reactive power optimization strategies solved by the three models.

	Active Power Strategy					Computation Time/s
	OLTC	**CB1/Set**	**CB2/Set**	*SVC1*/kVar	*SVC2*/kVar	
Deterministic model	0.975	3	5	432	738	1.92
Stochastic model	0.975	4	6	609	1079	205.13
Hybrid-driven model	0.975	4	6	586	1062	2.69

As can be seen in Table 4:

(1) Since the effect of source–load fluctuation was not considered, the strategy solved by the deterministic model was partially different compared to the other two models,

and the power compensation of each reactive power compensation device was smaller than the other two models.

(2)　Compared with the stochastic model, the reactive power strategy of the hybrid-driven model had completely consistent results for the discrete variables, and the maximum deviation of the continuous variable results was 3.78%, which shows that the hybrid-driven model has a similar level of solution performance as the stochastic optimization model in dealing with the source–load uncertainty.

(3)　In terms of computation rapidity, the computation time of the stochastic optimization model was 205.13 s due to the simulation of a large number of scenarios, while the computation time of the hybrid-driven model was 2.69 s, which is only 1.31% of that of the stochastic model, and only 0.77 s slower than that of the deterministic model, indicating that the hybrid-driven model can effectively ensure the rapidity requirement for online application.

Through the above analysis, the proposed hybrid-driven model was shown to have a similar solution performance as the stochastic optimization model, which ensures the reasonableness of the results. Additionally, the hybrid-driven model has obvious advantages in terms of calculation speed. Therefore, the hybrid-driven model is more suitable for real-time control of reactive power and voltage than the two traditional models.

2.　Analysis of the Adaptation to Source–load Uncertainty

To verify the adaptability of the proposed hybrid-driven model to source–load uncertainty, 30 groups of source and load data were randomly generated to simulate actual source–load fluctuation scenarios, in accordance with the predicted data and prediction error coefficients in Section 5.1. In each scenario, the power flow calculations were performed based on the reactive power strategies solved by the three models. Figures 4 and 5 show the voltage distribution and active power loss based on the power flow calculation, respectively. Different colors represent different simulation scenarios.

(a)

(b)

Figure 4. *Cont.*

(**c**)
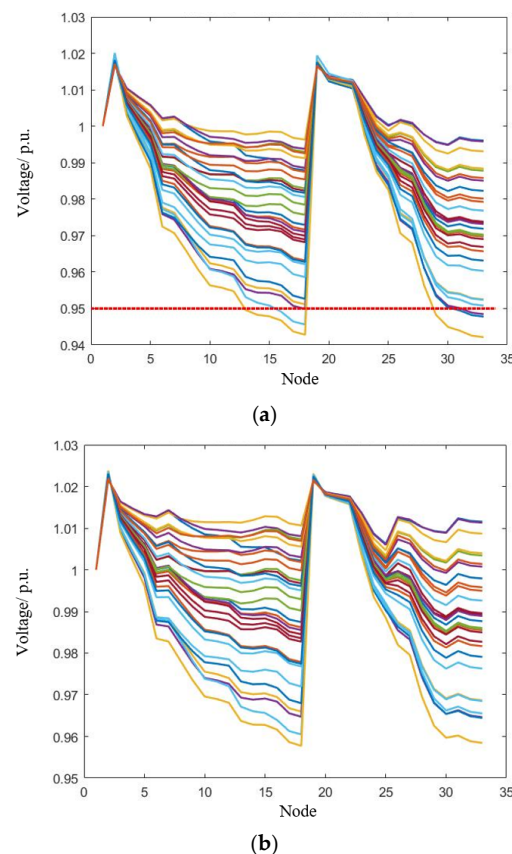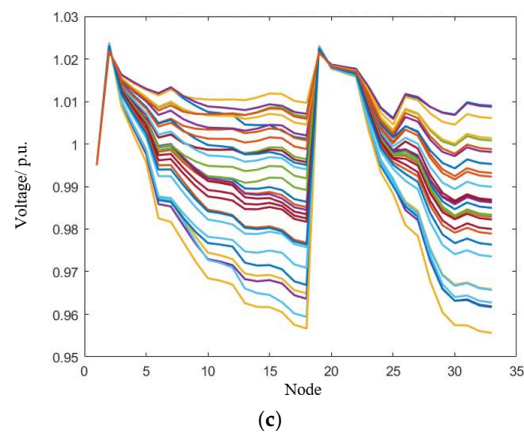
Figure 4. Comparison of voltage distribution of the three reactive power optimization strategies under different simulation scenarios. (**a**) voltage distribution of the deterministic optimization strategy; (**b**) voltage distribution of the stochastic optimization strategy; (**c**) voltage distribution of the hybrid-driven optimization strategy.
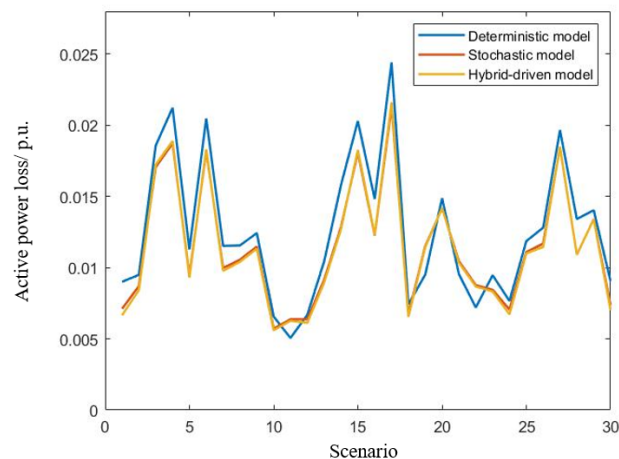
Figure 5. Comparison of active power loss of the three reactive power optimization strategies under different simulation scenarios.

As can be seen from the results of Table 5:

(1)　In all simulated source–load scenarios, the reactive power strategies of both the hybrid-driven model and the stochastic model did not lead to voltage violations, while the reactive power strategy of the deterministic model may lead to voltage exceeding the lower limits in the three scenarios, with the lowest voltage of 0.9428 p.u.

(2)　The average voltage expectation of the hybrid-driven model was improved by 1.56% and the average voltage offset expectation was decreased by 27.08% compared to the deterministic model. This indicates that the hybrid-driven model performs well in most scenarios.

(3)　In most scenarios, the active power loss values corresponding to both the stochastic model and hybrid-driven model were smaller than those of the deterministic model. However, in some scenarios, such as scenario 11, scenario 19, scenario 21 and scenario 22, the deterministic optimization model performed better. Through further analysis, the simulated source and load data in these four scenarios were close to the predicted data, which shows that the deterministic optimization strategy based on the predicted data performed better.

From the above analysis, it can be concluded that the reactive power strategy solved by the hybrid-driven model can effectively reduce the system active power loss in most source–load fluctuation scenarios, and show stronger adaptability to source–load uncertainty.

Table 5. Comparison of evaluation indexes of the three reactive power optimization strategies.

	Average Voltage Expectation/p.u.	Average Voltage Offset Expectation/p.u.	Number of Voltage Violations
Deterministic model	0.9821	1.662	3
Stochastic model	0.9982	1.208	–
Hybrid-driven model	0.9974	1.212	–

5.3. Analysis of the Influence of the Distributed Generation Prediction Error

In this section, the load prediction error coefficient was set to 5%, and the distributed generation prediction error coefficients were set to increments of 5% in turn. The deterministic model and the hybrid-driven model were used to solve the reactive power optimization separately. Based on the reactive power strategies obtained with different source–load prediction error coefficients, the power flow calculations were performed in 50 groups of randomly generated scenarios, and the results are shown in Table 6.

Table 6. Active power loss and voltage violation with different distributed generation prediction error coefficients.

		Distributed Generation Prediction Error Coefficients				
		5%	**10%**	**15%**	**20%**	**25%**
Active network loss expectation/kW	Deterministic model	105.6	117.2	144.3	182.1	162.7
	Hybrid-driven model	113.2	124.4	132.6	154.2	144.3
Number of Voltage violations	Deterministic model	–	–	3	5	8
	Hybrid-driven model	–	–	–	2	4

As can be seen in Table 6:

(1) When the prediction error coefficients of WT and PV output did not exceed 10%, the expected value of active power loss corresponding to the deterministic model optimization strategy was smaller than that of the hybrid-driven model. When the prediction error coefficients were greater than 10%, the expected value of active power loss corresponding to the deterministic model optimization strategy started to increase significantly, and was higher than that of the hybrid-driven model.

(2) When the prediction error coefficients reached 20%, the optimization strategy of the hybrid-driven model began to incur voltage violations in some scenarios. The deterministic model incurred voltage violations at the prediction error coefficient of 15%, with a much higher probability than the hybrid-driven model.

In summary, the hybrid-driven model showed better adaptability to both economy and security at different levels of prediction error coefficients. When the prediction error was large, the performance of the hybrid-driven model was more prominent.

6. Conclusions

This paper proposes a mechanism–data hybrid drive model for online voltage control. The mechanism-driven deterministic reactive power optimization strategy and the stochastic reactive power optimization strategy were used as training features and labels to train the CNN–GRU data-driven model, thus realizing the integration of mechanism and data. When applied online, the hybrid-driven model can enable fast correction of the reactive power strategy, effectively accounting for the influence of source–load uncertainty on real-time voltage control. As can be seen from the analysis:

(1) Compared with the stochastic optimization model, the proposed hybrid-driven model has outstanding advantages in terms of calculation speed, as it can significantly reduce the calculation time while ensuring the reasonableness of the results. Furthermore, compared with the deterministic optimization model, the hybrid-driven model has

outstanding advantages in terms of adaptability to source–load uncertainty, as it reduces the system active power loss and voltage violation risk to a certain extent. Therefore, the hybrid-driven model can effectively satisfy the requirements for online voltage control;

(2) Under different levels of distributed generation output prediction errors, the hybrid-driven model has excellent adaptability in terms of system economy and security. Therefore, it can be better applied to distribution system operation scenarios with large-scale distributed generations access.

Appendix A

Table A1. Line parameters of the case system.

Branch No.	From Node	To Node	Impedance (Ω)
1	1	2	0.0922 + j0.0470
2	2	3	0.4930 + j0.2511
3	3	4	0.3660 + j0.1864
4	4	5	0.3811 + j0.1941
5	5	6	0.8190 + j0.7070
6	6	7	0.1872 + j0.6188
7	7	8	0.7114 + j0.2351
8	8	9	1.0300 + j0.7400
9	9	10	1.0440 + j0.7400
10	10	11	0.1966 + j0.0650
11	11	12	0.3744 + j0.1238
12	12	13	1.4680 + j1.1550
13	13	14	0.5416 + j0.7129
14	14	15	0.5910 + j0.5260
15	15	16	0.7463 + j0.5450
16	16	17	1.2890 + j1.7210
17	17	18	0.7320 + j0.5740
18	2	19	0.1640 + j0.1565
19	19	20	1.5042 + j1.3554
20	20	21	0.4095 + j0.4784
21	21	22	0.7089 + j0.9373
22	3	23	0.4512 + j0.3083
23	23	24	0.8980 + j0.7091
24	24	25	0.8960 + j0.7011
25	6	26	0.2030 + j0.1034
26	26	27	0.2842 + j0.1447
27	27	28	1.0590 + j0.9337
28	28	29	0.8042 + j0.7006
29	29	30	0.5075 + j0.2585
30	30	31	0.9744 + j0.9630
31	31	32	0.3105 + j0.3619
32	32	33	0.3410 + j0.5362

References

1. Liu, J.; Zhang, Y. Has carbon emissions trading system promoted non-fossil energy development in China? *Appl. Energy* **2021**, *302*, 117613. [CrossRef]
2. Liu, W.; Zhan, J.; Chung, C.; Li, Y. Day-ahead optimal operation for multi-energy residential systems with renewables. *IEEE Trans. Sustain. Energy* **2018**, *10*, 1927–1938. [CrossRef]
3. Chen, S.; Hu, W.; Du, Y.; Wang, S.; Zhang, C.; Chen, Z. Three-stage relaxation-weightsum-correction based probabilistic reactive power optimization in the distribution network with multiple wind generators. *Int. J. Electr. Power Energy Syst.* **2022**, *141*, 108146. [CrossRef]
4. Wu, W.; Tian, Z.; Zhang, B. An Exact Linearization Method for OLTC of Transformer in Branch Flow Model. *IEEE Trans. Power Syst.* **2017**, *32*, 2475–2476. [CrossRef]
5. Li, P.; Jin, B.; Wang, D.; Zhang, B. Distribution system voltage control under uncertainties using tractable chance constraints. *IEEE Trans. Power Syst.* **2018**, *34*, 5208–5216. [CrossRef]
6. Biswas, P.; Suganthan, P.; Mallipeddi, R.; Amaratunga, G. Optimal reactive power dispatch with uncertainties in load demand and renewable energy sources adopting scenario-based approach. *Appl. Soft Comput.* **2019**, *75*, 616–632. [CrossRef]
7. Zhao, P.; Gu, C.; Xiang, Y.; Zhang, X.; Shen, Y.; Li, S. Reactive power optimization in integrated electricity and gas systems. *IEEE Syst. J.* **2020**, *15*, 2744–2754. [CrossRef]
8. Ding, T.; Liu, S.; Yuan, W.; Bie, Z.; Zeng, B. A Two-Stage Robust Reactive Power Optimization Considering Uncertain Wind Power Integration in Active Distribution Networks. *IEEE Trans. Sustain. Energy* **2016**, *7*, 301–311. [CrossRef]
9. Xu, Y.; Zhang, W.; Liu, W.; Ferrese, F. Multiagent-Based Reinforcement Learning for Optimal Reactive Power Dispatch. *IEEE Trans. Syst. Man Cybern. Part C* **2012**, *42*, 1742–1751. [CrossRef]
10. Liu, S.; Ding, C.; Wang, Y.; Zhang, Z.; Chu, M.; Wang, M. Deep Reinforcement Learning-Based Voltage Control Method for Distribution Network with High Penetration of Renewable Energy. In Proceedings of the 2021 IEEE Sustainable Power and Energy Conference (iSPEC), Nanjing, China, 23–25 December 2021.
11. Ding, T.; Yang, Q.; Yang, Y.; Li, C.; Bie, Z.; Blaabjerg, F. A Data-Driven Stochastic Reactive Power Optimization Considering Uncertainties in Active Distribution Networks and Decomposition Method. *IEEE Trans. Smart Grid* **2018**, *9*, 4994–5004. [CrossRef]
12. Sheng, W.; Liu, K.; Niu, H.; Zhao, J. The anomalous data identification study of reactive power optimization system based on big data. In Proceedings of the International Conference on Probabilistic Methods Applied to Power Systems, Beijing, China, 16–20 October 2016.
13. Cao, D.; Zhao, J.; Hu, W.; Ding, F.; Huang, Q.; Chen, Z.; Blaabjerg, F. Data-driven multi-agent deep reinforcement learning for distribution system decentralized voltage control with high penetration of PVs. *IEEE Trans. Smart Grid* **2021**, *12*, 4137–4150. [CrossRef]
14. Li, F.; Wang, Q.; Hu, J.; Tang, Y. Combined data-driven and knowledge-driven methodology research advances and its applied prospect in power systems. *Proc. CSEE* **2021**, *41*, 4377–4389.
15. Tan, Y.; Chen, Y.; Li, Y.; Cao, Y. Linearizing Power Flow Model: A Hybrid Physical Model-Driven and Data-Driven Approach. *IEEE Trans. Power Syst.* **2020**, *35*, 2475–2478. [CrossRef]
16. Li, M.; Zheng, Y.; Tang, B.; Yu, G.; Wang, Z.; Muyeen, S.M. A Failure Assessment Method of Island Distribution Lines Based on Model-Data Hybrid Drive. *IET Gener. Transm. Distrib.* **2022**, *16*, 4867–4877. [CrossRef]
17. Wang, Q.; Li, F.; Tang, Y.; Xu, Y. Integrating model-driven and data-driven methods for power system frequency stability assessment and control. *IEEE Trans. Power Syst.* **2019**, *34*, 4557–4568. [CrossRef]
18. Tian, H.; Zhao, H.; Liu, C.; Chen, J.; Wu, Q.; Terzija, V. A dual-driven linear modeling approach for multiple energy flow calculation in electricity–heat system. *Appl. Energy* **2022**, *314*, 118872. [CrossRef]
19. Sharma, S.; Verma, A.; Xu, Y.; Panigrahi, B. Robustly coordinated bi-level energy management of a multi-energy building under multiple uncertainties. *IEEE Trans. Sustain. Energy* **2019**, *12*, 3–13. [CrossRef]
20. Su, P.; Liu, T.; Li, X. Determination of Optimal Spinning Reserve of Power Grid Containing Wind. *Power Syst. Technol.* **2010**, *34*, 158–162.
21. Mohseni-Bonab, S.M.; Rabiee, A.; Mohammadi-Ivatloo, B.; Jalilzadeh, S.; Nojavan, S. A two-point estimate method for uncertainty modeling in multi-objective optimal reactive power dispatch problem. *Int. J. Electr. Power Energy Syst.* **2016**, *75*, 194–204. [CrossRef]
22. Li, K.; Wang, R.; Lei, H.; Zhang, T.; Liu, Y.; Zheng, X. Interval prediction of solar power using an improved bootstrap method. *Sol. Energy* **2018**, *159*, 97–112. [CrossRef]
23. Lee, Y.; Scholtes, S. Empirical prediction intervals revisited. *Int. J. Forecast.* **2014**, *30*, 217–234. [CrossRef]
24. Xiao, T.; Pei, W.; Chen, N.; Wang, X.; Pu, T. Maximum operation duration assessment of isolated island considering the uncertainty of load reduction capability of air conditioner. *Proc. CSEE* **2019**, *39*, 4982–4994.
25. Kabir, M.; Mishra, Y.; Bansal, R. Probabilistic load flow for distribution systems with uncertain PV generation. *Appl. Energy* **2016**, *163*, 343–351. [CrossRef]
26. Gao, H.; Liu, J.; Wang, L. Robust Coordinated Optimization of Active and Reactive Power in Active Distribution Systems. *IEEE Trans. Smart Grid* **2018**, *9*, 4436–4447. [CrossRef]
27. Sun, X.; Qiu, J.; Tao, Y.; Ma, Y.; Zhao, J. A multi-mode data-driven volt/var control strategy with conservation voltage reduction in active distribution networks. *IEEE Trans. Sustain. Energy* **2022**, *13*, 1073–1085. [CrossRef]

28. Sajjad, M.; Khan, Z.A.; Ullah, A.; Hussain, T.; Ullah, W.; Lee, M.Y.; Baik, S.W. A novel CNN-GRU-based hybrid approach for short-term residential load forecasting. *IEEE Access* **2020**, *8*, 143759–143768. [CrossRef]
29. Shao, M.; Wu, J.; Shi, C.; An, R.; Zhu, X.; Huang, X.; Cai, R. Reactive power optimization of distribution network based on data driven and deep belief network. *Power Syst. Technol.* **2019**, *43*, 1874–1885.
30. Baran, M.E.; Wu, F.F. Network reconfiguration in distribution systems for loss reduction and load balancing. *IEEE Trans. Power Deliv.* **1989**, *4*, 1401–1407. [CrossRef]